FEBS J. Author manuscript; available in PMC 2016 December 06.

Published in final edited form as:

FEBS J. 2009 January ; 276(2): 479–496. doi:10.1111/j.1742-4658.2008.06797.x.

Characterization of a monoclonal antibody as the first specific inhibitor of human NTP diphosphohydrolase-3:

Partial characterization of the inhibitory epitope and potential applications

Mercedes N. Munkonda[1], **Julie Pelletier**[1], **Vasily V. Ivanenkov**[2], **Michel Fausther**[1], **Alain Tremblay**[1], **Beat Künzli**[3], **Terence L. Kirley**[2], and **Jean Sévigny**[1]

[1]Centre de Recherche en Rhumatologie et Immunologie, Centre Hospitalier Universitaire de Québec, Université Laval, Canada

[2]Department of Pharmacology and Cell Biophysics, College of Medicine, University of Cincinnati, OH, USA

[3]Department of General Surgery, Universität München, Germany

Abstract

The study and therapeutic modulation of purinergic signaling is hindered by a lack of specific inhibitors for NTP diphosphohydrolases (NTPDases), which are the terminating enzymes for these processes. In addition, little is known of the NTPDase protein structural elements that affect enzymatic activity and which could be used as targets for inhibitor design. In the present study, we report the first inhibitory monoclonal antibodies specific for an NTPDase, namely human NTPDase3 (EC 3.6.1.5), as assessed by ELISA, western blotting, flow cytometry, immunohistochemistry and inhibition assays. Antibody recognition of NTPDase3 is greatly attenuated by denaturation with SDS, and abolished by reducing agents, indicating the significance of the native conformation and the disulfide bonds for epitope recognition. Using site-directed chemical cleavage, the SDS-resistant parts of the epitope were located in two fragments of the C-terminal lobe of NTPDase3 (i.e. Leu220–Cys347 and Cys347–Pro485), which are both required for antibody binding. Additional site-directed mutagenesis revealed the importance of Ser297 and the fifth disulfide bond (Cys399–Cys422) for antibody binding, indicating that the discontinuous inhibitory epitope is located on the extracellular C-terminal lobe of NTPDase3. These antibodies inhibit recombinant NTPDase3 by 60–90%, depending on the conditions. More importantly, they also efficiently inhibit the NTPDase3 expressed in insulin secreting human pancreatic islet cells *in situ*. Because insulin secretion is modulated by extracellular ATP and purinergic receptors, this finding suggests the potential application of these inhibitory antibodies for the study and control of insulin secretion.

Keywords

ATP; immunological techniques; inhibitor; monoclonal antibody; NTPDase

Correspondence: J. Sévigny, Centre de Recherche en Rhumatologie et Immunologie, Centre Hospitalier Universitaire de Québec (CHUQ), 2705 Boulevard Laurier local T1-49, Québec, QC G1V 4G2, Canada, Fax: +1 418 654 2765, Tel: +1 418 654 2772, jean.sevigny@crchul.ulaval.ca.

Plasma membrane-bound nucleoside triphosphate diphosphohydrolase-1, 2, 3 and 8 (NTPDase1, 2, 3 and 8) control nucleotide levels at the cell surface by hydrolyzing the γ and β phosphates of nucleotides [1,2]. These enzymes appear to play key roles in the modulation and termination of P2 receptor signaling, as demonstrated for NTPDase1 and NTPDase2 [3–10]. Other NTPDases, such as NTPDase4, 5, 6 and 7, are mainly associated with the membranes of intracellular organelles, and therefore are not expected to play a major role in P2 receptor signaling [1]. The variable ability of the cell surface NTPDases to hydrolyze nucleoside triphosphates (e.g. ATP) and diphosphates (e.g. ADP), coupled with the distinct affinities of the nucleotide NTPDase substrates and products for different purinergic receptor subtypes, are expected to dictate distinct physiological functions for each NTPDase [1,2].

The elucidation of the physiological roles of the NTPDases has been hampered by the lack of specific inhibitors. The few biological roles for individual NTPDases described so far have been suggested by studies using genetically modified animals and ‘knockdown’ systems, or inferred from sites of localization of expression. For example, knockout mice deficient in NTPDase1 expression exhibited a major perturbation of P2 receptor signaling, resulting in disordered regulation of inflammation and blood coagulation in several animal models [3–5,8–10]. These effects were associated with dysfunction of vascular endothelial cells, monocytes, dendritic cells and platelets in NTPDase1 ablated mice. Imai *et al.* [11] reported the specific inhibition of human NTPDase1 with oligonucleotides, but this finding has not been refined further in any subsequent studies. Using siRNA, Jhandier *et al.* [7] proposed a function for NTPDase2 in the proliferation of cholangiocytes. A role for NTPDase2 in the regulation of stem and progenitor cells proliferation in mammalian brain has also been inferred recently [12].

The function of NTPDase3 (EC 3.6.1.5) has not been clearly established, due, in part, to a lack of a specific inhibitor. In addition to the termination of P2 receptor signaling specific for ATP and UTP, NTPDase3 may transiently activate other P2 nucleotide receptors because it generates a transient accumulation of ADP and/or UDP [2,13]. In concert with ecto-5′-nucleotidase, NTPDase3 also generates adenosine, which activates P1 receptors [2,13]. Immunolocalization of NTPDase3 in the rat brain has demonstrated that expression is mostly restricted to axons and is associated with synapse-like structures, suggesting that the enzyme acts as a regulator of synaptic function. Its pattern of expression in hypocretin-1/orexin-A positive cells of the hypothalamus suggested that NTPDase3 may modulate feeding, the sleep/wake cycle and other behaviors controlled by diverse homeostatic systems present in this brain region [14,15]. In the zebrafish, NTPDase3 was also localized to the hypothalamus, as well as to cranial nerves and primary sensory nerves of the spinal cord [16]. Vlajkovic *et al.* [17] reported NTPDase3 immunoreactivity in the primary afferent neurons of the spiral ganglion and synaptic regions of the inner and outer hair cells of the rat cochlea, suggesting a role for NTPDase3 in auditory neurotransmission. In the rat kidney, NTPDase3 was immunolocalized in all post-proximal nephron segments examined, but no function has been attributed to the enzyme so far [18]. The cellular localization of NTPDase3 in other tissues has not yet been reported.

Although there are few nucleotide analogs and other chemicals that have been reported to inhibit NTPDase activities [19–23], they are either not completely specific for NTPDases, or

their specificities have not been clearly established. We previously generated a series of specific antibodies to NTPDase3 of different species: antibodies to human NTPDase3, namely KLH1 [24], KLH11 and KLH12 [25]; antibodies to mouse NTPDase3, namely KLH7, KLH15 [15] and mN3-3_C [26]; and antibodies to rat NTPDase3, namely KLH14 [15], rN3-1_L [18] and rN3-3_L [27]. All of these antibodies are polyclonals, and none are inhibitory. In the present study, we generated monoclonal antibodies against human NTPDase3, and provide evidence that these antibodies are efficient and selective inhibitors of this NTPDase isoform and are also applicable to various immunological techniques. Based on data obtained in the present study indicating that NTPDase3 is expressed by pancreatic islet cells, which secrete insulin, as well as on previous findings demonstrating that insulin secretion by these cells is modulated by extracellular ATP via purinergic receptors [28–30], the inhibitory monoclonal antibodies generated and characterized in the present study are shown not only to be useful biochemical tools for studying the structure and function of NTPDase3, but also comprise potential therapeutic agents that may effectively modulate insulin secretion, which may even prove useful for the study and treatment of diabetes.

Interestingly, the identification of the inhibitory epitope may lead to hypotheses concerning the mechanism of inhibition by the antibodies, as well as to experimental refinements yielding more efficient inhibitory antibodies and the design of antibodies specific for the inhibition of other NTPDase enzyme family members. The latter advance would be based on the assumption that different antibodies binding specifically to the regions of other NTPDases that are homologous to the identified NTPDase3 inhibitory epitope will specifically inhibit those other NTPDases. Thus, the extension of such a study may lead to the generation of inhibitory antibodies to other NTPDases, which would prove useful in further studies and have potential therapeutic application via modulation of purinergic signaling. For all these reasons, we also attempted to define the inhibitory epitope on human NTPDase3.

Results

Antibody production

Hybridomas were generated from B-cells from BALB/c mice injected with wild-type human NTPDase3 cDNA (in pcDNA3 vector). A final boost injection was made using intact human embryonic kidney (HEK) 293T cells transfected with the above human NTPDase3 expression vector. The positive hybridomas were screened by ELISA using human NTPDase3 expressing COS-7 cells fixed to the wells. Two hybridomas, hN3-$B3_S$ and hN3-$H10_S$, produced a positive response using transfected cells and a negative one using nontransfected cells, and were subsequently cloned and analysed. The isotypes of the antibodies produced by these hybridomas were determined by dot blot using rat monoclonal antibodies specific for different mouse immunoglobulin isotypes. Both hN3-$B3_S$ and hN3-$H10_S$ produced IgG with γ2b heavy chains (data not shown).

Antibody specificity

The monoclonal antibodies hN3-B3$_S$ and hN3-H10$_S$ specifically recognize recombinant human NTPDase3—The specificity of hN3-B3$_S$ and hN3-H10$_S$ antibodies were tested by western blot, flow cytometry and immunocytochemistry, using recombinant NTPDases expressed transiently in COS-7 cells. As illustrated by the western blots shown in Fig. 1A, the expected protein bands corresponding to the monomeric (75 kDa) and the dimeric (150 kDa) forms of human NTPDase3 were detected by both antibodies in the cell extracts from human NTPDase3 transfected COS-7 cells. All other cell extracts from either nontransfected COS-7 cells or cells transfected with mouse or rat NTPDase3, or with any other plasma membrane localized human NTPDase1, 2 or 8, were all negative.

Flow cytometry and immunocytochemistry confirmed the specificity of the reaction of hN3-B3$_S$ and hN3-H10$_S$ because a strong positive signal could only be detected in human NTPDase3 transfected cells (Fig. 1B,C). No signal was detected in nontransfected COS-7 cells with either of these monoclonal antibodies. These data indicate that both of these monoclonal antibodies detect the native human NTPDase3 protein.

hN3-B3$_S$ and hN3-H10$_S$ specifically inhibit the biochemical activity of recombinant human NTPDase3—The effect of both hN3-B3$_S$ and hN3-H10$_S$ binding to human NTPDase3 on its biochemical activity was first tested with crude cell membranes from transfected COS-7 cells in three different buffers. Although the IC_{50} determined in both the calcium and the magnesium buffers was lower, a maximal inhibition of 87% was reached with the modified Ringer buffer (Fig. 2A), which was used for the other assays. Figure 2B,C shows that both monoclonal antibodies inhibited human NTPDase3 significantly, and at a similar level, in a dose-dependent manner, with either ATP or ADP as substrates. In these conditions, hN3-B3$_S$ inhibited ATPase and ADPase activity of human NTPDase3 by 76 ± 9% and 72 ± 9%, respectively, and hN3-H10$_S$ by 76 ± 10% and 77 ± 12%, respectively (mean ± SEM, $n = 9$; Fig. 2C). Using a fixed concentration of the inhibitory antibodies (1.35 nM) to give a maximal inhibition, the extent of inhibition did not vary with ATP concentrations varying from below the K_M value (10 μM) to far above it (750 μM; data not shown). In addition, the monoclonal antibodies also effectively inhibited, although to a lesser extent, the ATPase activity of NTPDase3 at the surface of intact transfected COS-7 cells (Fig. 2D).

Because hN3-B3$_S$ and hN3-H10$_S$ antibodies were specific for human NTPDase3 on western blot, we investigated whether the inhibition of human NTPDase3 was also specific. Therefore, these monoclonal antibodies were incubated with cell extracts from the recombinant forms of the other human plasma membrane bound NTPDases (NTPDase1, 2 and 8) prior to ATP hydrolysis assays. Neither of these human NTPDases (Fig. 2E), nor rat or mouse NTPDase3 (data not shown), were inhibited by hN3-B3$_S$ or hN3-H10$_S$. In these assays, a monoclonal antibody specific for cytohesin (6D4-4) was used as a negative control.

NTPDase3 localization and specific inhibition in human pancreas sections—We previously reported the localization of NTPDase3 in Langerhans ilets of mouse pancreas

[31]. In addition, human pancreas was shown to express NTPDase3 mRNA [32]. Using the generated monoclonal antibodies, NTPDase3 expression was also located in Langerhans islet cells in humans (Fig. 3B). By contrast, NTPDase1 was detected in the vasculature and in acini (Fig. 3A), as expected from previous studies [33].

Accordingly, we then tested the ability of hN3-H10$_S$ to inhibit the native human NTPDase3 *in situ*, using ATP as substrate and a histochemical method (Fig. 3C–H). In the absence of the monoclonal antibody, ATPase activity was detected mainly in Langerhans islets and in blood vessels (Fig. 3D,E,G), in agreement with NTPDase1 and NTPDase3 expression. After pre-incubation of the pancreas sections with hN3-H10$_S$ antibody, the ecto-ATPase activity was significantly reduced in Langerhans islets but not in blood vessels (Fig. 3F,H). Controls using pancreas sections pre-incubated with unrelated, purified mouse IgGs antibodies did not affect the ATPase activity (Fig. 3E), giving a reaction similar to that in the other controls (Fig. 3D,G). Taken together, these results indicate that the monoclonal antibody hN3-H10$_S$ specifically inhibits human pancreatic islet cell NTPDase3 activity *in situ*.

Epitope characterization and mapping

Site-directed cleavage of human NTPDase3 with 2-nitro-5-thiocyanatobenzoic acid (NTCB)—To approximately locate the antibody epitope in the primary structure, we cleaved NTPDase3 at several sites and analyzed antibody binding to the fragments by western blotting under nonreducing conditions. Site-directed cleavage was achieved by introduction of cysteine residues via mutagenesis at strategic positions, and subsequent chemical cleavage at the introduced cysteine residues using the NTCB reagent [34]. Only highly reactive cysteines (as demonstrated by alkylation and other modifications; data not shown) were substantially cleaved by NTCB under nondenaturing conditions, whereas less reactive cysteines were poorly hydrolyzed. Supplementing 1 M glycine as a nucleophile to optimize the cleavage efficiency [35], or performing the reaction under denaturing conditions (in 8 M urea, or in SDS 0.04–1%), did not increase the efficiency of cleavage (data not shown). Four mutations (i.e. L218C, L220C, C347S and C353S) produced substantial cleavage. All of them were made in a C10S hNTPDase3 background to avoid the problem of intermolecular disulfide formation via C10, which occurs during cell membrane preparation of human NTPDase3 [36]. Mutations L218C and L220C replaced Leu by Cys in apyrase conserved region (ACR) 4 (where L220 corresponds to the ‘X’ in the (219)DXG(221) conserved motif), whereas mutations C347S and C353S disrupted the non-essential fourth disulfide bond (C347-S-S-C353) and, thus, created a nonpaired cysteine for NTCB reaction and cleavage. These NTPDase3 mutants had specific nucleotidase activities similar to the wild-type-like C10S NTPDase3 used as a background for the mutations (data not shown).

Cleavage with NTCB at residues L218C and L220C produced a fragment of approximately 48 kDa, which bound monoclonal antibody as efficiently as the noncleaved protein, as assessed by comparing the relative western blot reactivity of KLH11 with the monoclonal antibodies (Fig. 4A). This locates the monoclonal antibody epitope within the C-terminal half of the protein starting at residue Leu220 of the wild-type NTPDase3 (Fig. 8A).

Cleavage with NTCB at residues C347 or C353 produced two fragments of approximately 30 and 42 kDa, respectively, neither of which is recognized by the monoclonal antibodies (Fig. 4B). This suggests that cleavage at residue C347 or C353 splits the epitope, and that both of these parts are required for binding monoclonal antibody after SDS denaturation and western blotting (Fig. 8A).

Competition of the monoclonal antibody hN3-H10$_S$ with polyclonal antibodies KLH11 and KLH12—Peptide sequences recognized by KLH11 [(311)Asp-Gly(327)] and KLH12 [(265)Asn-Thr(281)] polyclonal antibodies are included in the same fragment containing the monoclonal antibody epitope (Fig. 8A). Therefore, we investigated whether the monoclonal epitope overlaps either KLH11 or KLH12 peptide epitopes (Fig. 5). Pre-incubation of western blots with KLH11 or KLH12 antibodies at high concentrations did not affect monoclonal antibody binding (Fig. 5), suggesting that the monoclonal antibody epitope does not overlap with KLH11 or KLH12 peptide epitopes.

Effect of single amino acid substitutions on binding monoclonal antibody—NTPDase3 mutants T286C, S295C, S297C and T299C were made in a C10S hNTPDase3 background. These mutants all showed essentially the same specific nucleotidase activity and expression level as the C10S NTPDase3 used as the background for the mutations, as determined by enzyme assays and western blots using the KLH1 antibody (data not shown). However, probing the nonreduced western blot of these mutants with the monoclonal antibodies demonstrated a greatly reduced antibody binding to S297C compared to other mutants (Fig. 6A). This suggests that Ser297 is included in a part of the monoclonal antibody epitope, and that this residue may be directly involved in binding the monoclonal antibody. Additional evidence in support of Ser297 being located in the epitope was obtained by measuring the decreased extent of inhibition of S297C Ca-ATPase activity by the monoclonal antibodies compared to the neighboring S295C and T299C mutations and the C10S NTPDase3 background (Fig. 6B).

Effect of individual disulfide bond disruption on the interaction of the inhibitory monoclonal antibody with native NTPDase3—We noted that SDS denaturation decreased binding of the antibodies because both monoclonal antibodies reacted much more strongly with NTPDase3 that was bound to poly(vinylidene difluoride) (PVDF) or nitrocellulose membranes under native conditions (i.e. by filtration of native COS cell membranes diluted in NaCl/Tris buffer through the membranes via slot blotting), as opposed to western blotted, SDS denatured protein. Thus, the detection limit for NTPDase3 on dot or slot blots is approximately 50–100-fold lower than that observed for western blots (data not shown). In addition, both inhibitory monoclonal antibodies do not recognize human NTPDase3 on western blots if the protein is reduced with dithiothreitol prior to SDS/PAGE. Thus, one or more of the five extracellular disulfide bonds in NTPDase3 [25] are required to maintain the epitope recognized by the monoclonal antibodies in the SDS denatured enzyme. We attempted to determine the importance of each of the five disulfide bonds for monoclonal antibody binding using the previously reported mutated forms of the enzyme [25]. As the amount of properly folded NTPDase3 protein produced upon expression of mutants lacking one of the five disulfide bonds varies considerably, we used

endo-β-*N*-acetylglucosaminidase digestion to estimate the amount of properly folded NTPDase3 in the samples. Endo-β-*N*-acetylglucosaminidase specifically recognizes and hydrolyzes highmannose glycans [37], which are characteristic of immature proteins resident in the endoplasmic reticulum [38]. Thus, treatment with endo-β-*N*-acetylglucosaminidase decreases the size of misfolded NTPDase3 protein to that of the nonglycosylated core protein, whereas the size of the properly folded and normally processed molecules decreases only slightly [25]. Therefore, the amount of properly folded NTPDase3 protein in each sample can be estimated by quantifying the western blot signal remaining at approximately 70 kDa after digestion by endo-β-*N*-acetylglucosaminidase (Fig. 7A). With this information, amounts of COS cell membranes that contain known amounts of properly folded NTPDase3 protein were applied to slot blots, and the resultant hN3-B3$_S$ monoclonal antibody signals were quantified (Fig. 7B). These results indicate that the monoclonal antibody reactivity to native NTPDase3 is not adversely affected by disruption of the first, second or fourth disulfide bond, but is decreased by approximately 87% by elimination of the fifth disulfide bond [immunoreactivity (density/properly folded protein); Fig. 7B]. Comparable results were obtained with the hN3-H10$_S$ antibody (data not shown). Because there is no properly folded protein in mutants lacking the third disulfide bond (Fig. 7A) [25], no conclusions can be made regarding the importance of this bond for monoclonal antibody reactivity against the native protein.

Discussion

We have previously described polyclonal antibodies that recognize either human, rat or mouse NTPDase3. These antibodies were useful for western blot and some of them also for immunohistological localization [15,18,24–27]. In the present study, we generated two hybridomas that produced IgG2b monoclonal antibodies specific for human NTPDase3, namely hN3-B3$_S$ and hN3-H10$_S$. These monoclonal antibodies are efficient in all the techniques tested in the present study, but only in nonreduced conditions: western and slot blots, ELISA, flow cytometry, immunocytochemistry and immunohistochemistry. The detection of monomeric (75 kDa) and dimeric (150 kDa) forms of NTPDase3 by the monoclonal antibodies is consistent with previously published studies of this enzyme [13,27,39]. Importantly, the biochemical activity of human NTPDase3 is specifically inhibited by the binding of either one of these two monoclonal antibodies; either in biochemical assays with the recombinant enzyme using intact cells or membranes from NTPDase3-transfected cells, or *in situ* as assessed in human pancreatic tissue sections. The extent of inhibition by the monoclonal antibodies did not vary with substrate concentration, suggesting that the mechanism of inhibition of the monoclonal antibodies is not via steric hindrance of the substrate for the active site, but may be due to restriction of enzyme lobe movements or deformation of the active site. Taken together, these experiments demonstrate that the monoclonal antibodies hN3-B3$_S$ and hN3-H10$_S$ recognize the native form of human NTPDase3. These two hybridomas may originate from the same B cell clone because all experiments performed yielded similar results using either antibody.

NTPDase3, as well as the other cell surface ectonucleotidase isoenzymes (i.e. NTPDase1, 2 and 8), most likely play an important role in the termination and modulation of P2 receptor signaling via hydrolysis of the agonists ATP, ADP, UTP and/or UDP [1]. The differential

ability of these NTPDase isozymes to hydrolyze these different nucleotides may define distinct roles in purinergic signaling processes. NTPDase1 hydrolyzes tri- and diphosphonucleosides equally well, whereas NTPDase2 prefers triphosphonucleosides. NTPDase3 and NTPDase8 have intermediate diversus trinucleoside specificity, and cause a less distinct transient accumulation of diphosphonucleosides than NTPDase2, which may promote the activation of ADP or UDP specific purinergic receptors ($P2Y_{1,6,12,13}$) [2].

The study of the biological functions under the control of proteins responsible for nucleotide release, binding and hydrolysis would greatly benefit from the availability of specific inhibitors of the various NTPDases. In addition, inhibition of the NTPDase nucleotide hydrolyzing enzymes would potentiate nucleotide signaling, and therefore could be used to modulate purinergic receptor signaling and the physiological processes under extracellular nucleotide control.

Two groups of molecules have been reported to inhibit NTPDases: (a) nucleotides and analogs, such as 8-BuS-ATP and ARL 67156, and (b) sulfonated dyes, such as Reactive Blue 2, suramin and derivatives [20,21,40,41]. 8-BuS-ATP has been poorly characterized and its specificity is not known. ARL 67156 is a weak inhibitor of NTPDase1 and NTPDase3 [23]. Suramin, Reactive Blue 2, NF279, NF449 and polyoxometalates have been described as potent micromolar selective inhibitors of human and murine NTPDase1, 2, 3 and 8 [21,22,42], but most of these compounds are also antagonists of P2 receptors. The most commonly used inhibitor of NTPDases in the past was sodium azide at high concentrations (5–20 mM) [43–45]. Sodium azide has been reported to inhibit the purified and recombinant form of several mammalian NTPDase1 enzymes, including bovine [46,47], porcine [48,49], human [50,51], rat [51] and mouse [52] NTPDase1. Human NTPDase3 is also inhibited by millimolar concentrations of azide [24]. By contrast, human, porcine, rat and mouse NTPDase8 are more resistant to inhibition by sodium azide [48,51]. However, azide is not specific for NTPDases because it inhibits mitochondrial ATPase at a much lower concentration. A very recent study described the synthesis of a uridine-5′-carboxamide derivative as the first potent and selective competitive inhibitor of human NTPDase2. This nucleotide analog had a K_i value of 8 μM and showed selectivity versus other NTPDases [53]. Thus, with the exception of the later molecule, there are no other specific inhibitors for NTPDases available to date and none that can clearly discriminate between the different isotypes. This complicates the determination of specific NTPDase functions, as well as the determination of the functions of the nucleotide receptors that they modulate. Therefore, the identification of monoclonal antibodies developed in the present study as specific inhibitors of human NTPDase3 is of significant value.

We also performed several experiments to locate parts of the discontinuous epitope of these inhibitory monoclonal antibodies. Because the structure of NTPDases appears to be well conserved, the identification of this epitope may prove useful for the future generation of novel and specific inhibitors of the other NTPDases. It should be noted that this high affinity epitope is present only in the native form of human NTPDase3. In addition, the reduction of disulfide bonds in NTPDase3 prevents interaction with the inhibitory monoclonal antibodies on western blots. Consequently, all western blot experiments utilizing the monoclonal antibodies were performed under nonreducing conditions. The monoclonal antibodies also

do not react with misfolded NTPDase3 on western blots, even under non-reducing conditions, as demonstrated by the lack of detection of the large aggregates of NTPDase3 (data not shown). Consequently, only natively folded and properly processed NTPDase3 can be used for monoclonal antibody epitope mapping. This restriction prevents use of the common epitope mapping approach for making truncated proteins because truncation of anything more than the short C-terminal cytoplasmic tail portion (i.e. the A511Stop mutant) [54] results in NTPDase3 proteins that are misfolded and enzymatically inactive, and thus not recognized by the inhibitory monoclonal antibodies (data not shown). Therefore, we used two other approaches to define the monoclonal antibody epitope: (a) introduction of cysteine residues by mutagenesis followed by chemical cleavage of native NTPDase3 with NTCB at the introduced residues and (b) disruption of individual disulfide bonds by mutagenesis. In addition, we analyzed the effect of point mutations on antibody binding, as well as the competition of existing polyclonal antibodies with the new monoclonal antibodies, to check for overlapping epitopes on NTPDase3.

Our monoclonal antibody epitope mapping data led to the following conclusions. First, the epitope is discontinuous and consists of at least three parts. One part of the epitope is disrupted during denaturation with SDS under nonreducing conditions. The structural features of that part are not known, but its disruption greatly reduces the strength of interaction with monoclonal antibody, as demonstrated by the much stronger reactivity of the monoclonals with native NTPDase3 on slot blots as opposed to denatured NTPDase3 on western blots. In addition, the high apparent affinity of the monoclonals for the native protein calculated from the inhibition of native NTPDase3 as a function of antibody concentration (Fig. 2A,B) would suggest a tight association with native NTPDase3. Second, the SDS-resistant parts of the epitope are located on two fragments of the extracellular C-terminal lobe, both of which are required for monoclonal antibody binding to denatured protein on western bot. In the L220-C347 fragment, Ser297 is likely to be a part of the epitope. In the C347-P485 fragment, the principal part of the epitope is likely located near the fifth disulfide bond because the disruption of this bond by mutagenesis dramatically reduces the strength of interaction of the native protein with the monoclonal antibodies (Fig. 7B). These data and conclusions are depicted schematically in Fig. 8A, and superimposed on a 3D model of the extracellular portion of hNTPDase3 in Fig. 8B, showing the location of Ser297, the fifth disulfide bond, and the fifth disulfide bond loop in the C-terminal lobe of the enzyme. These antibody epitope elements are located outside the active site, part of which is denoted in blue space-filling mode indicating the two ‘DXG’ motifs of the ACR1 and ACR4 (Fig. 8B) shown to surround the nucleotide substrate in the active site of the NTPDases [55]. Non-active site binding of the inhibitory antibodies is reasonable because the inhibitory monoclonal NTPDase3 antibodies described in the present study are both species and isotype specific, and the amino acid sequences (ACR sequences), and presumably the 3D structures, of the NTPDase active sites are well conserved among species and NTPDase isotypes.

In summary, we have generated monoclonal antibodies that are the first specific inhibitors of human NTPDase3. We partially defined their discontinuous epitope. These monoclonal antibodies are useful tools for immunological techniques and as specific inhibitors but, in addition, they may also lead to a better understanding of how to modulate the active site of

NTPDases, as well as identify a region of these enzymes that can be targeted to develop inhibitors specific for NTPDases other than human NTPDase3. Finally, we have also demonstrated a specific inhibition of ATPase activity of NTPDase3 in Langerhans islet cells of the human pancreas. The function of NTPDase3 in these cells is not yet well understood, and is currently under investigation [56]. However, because islet cells secrete insulin, and the secretion of insulin is altered by extracellular ATP via purinergic receptors and signaling [28–30], these monoclonal antibodies may be useful for controlling insulin secretion and the biological and pathological processes modulated by insulin.

Experimental procedures

Materials

Aprotinin, nucleotides, phenylmethanesulfonyl fluoride, tetrabutylammonium hydrogen sulfate, sodium deoxycholate, NTCB and malachite green were purchased from Sigma-Aldrich (St Louis, MO, USA). Tris was provided by VWR International (Montreal, Canada) and Bis-Tris was obtained from EMD Chemicals (Gibbstown, NJ, USA). DMEM was obtained from Invitrogen (Burlington, Canada), Fetal bovine serum and antibiotic-antimycotic solution were obtained from Wisent (St-Bruno, Canada), and hematoxylin was obtained from Biomeda Corporation (Foster City, CA, USA).

Plasmids

The plasmids have been previously described: human NTPDase1 (GenBank accession no. U87967) [57], human NTPDase3 (AF034840) [24], human NTPDase8 (AY430414) [51] and mouse NTPDase3 (AY376710) [13]. Human NTPDase2 (NM_001246) [58] and rat NTPDase3 (NM_178106) [27] were kindly provided by A. Knowles (San Diego State University, CA, USA) and H. Zimmermann (J. W. Goethe University, Frankfurt am Main, Germany), respectively.

Generation of hybridomas

Two BALB/c mice were immunized by intradermal and intramuscular injection of 100 μg of plasmid encoding human NTPDase3 dissolved in NaCl/P_i at weeks 0, 2, 4, 12 and 20. The mouse whose serum had the highest titer after the last injection of the plasmid, as determined by western blot under nonreduced conditions, received a final intraperitoneal injection of 10^7 HEK 293T cells transfected with human NTPDase3 at week 46. Three days later, the spleen was collected for the production of hybridomas. Myeloma SP2/0 cells were grown in DMEM containing high glucose and supplemented with 10% fetal bovine serum and 1 × antibiotic-antimycotic (1000 units of penicillin, 1 mg of streptomycin and 0.25 μg of amphotericin B per mL of 0.85% saline; Invitrogen). For fusion, SP2/0 cells were centrifuged, resuspended in DMEM, and combined with splenocytes at a ratio of 1 : 10. After centrifugation at 300 ***g*** for 10 min at room temperature, cells were resuspended in 1 mL of polyethylene glycol solution (50%, w/v; MW 1450 in Dulbecco's NaCl/P_i without calcium), and distributed in 96-well plates. After hypoxanthine/aminopterin/thymidine medium selection, supernatants were tested by ELISA. Positive hybridomas were cloned by limiting dilution using hypoxanthine/thymidine medium instead of hypoxanthine/aminopterin/thymidine medium, cultured and frozen.

ELISA

ELISA was performed on COS-7 cells transfected with human NTPDase3. One day after transfection, cells were trypsinized and transferred to 96-well plates. The next day, cells were washed twice with NaCl/P_i-Tween and fixed for 2 min in a cold solution containing 95% acetone (Fisher Scientific Co., Ottawa, Canada) and 5% of a 10% formalin solution (Fisher Scientific Co.). Washed cells were incubated in a blocking solution (0.5% bovine serum albumin in NaCl/P_i-Tween) for 2 h at room temperature. The blocking solution was removed and the supernatant of hybridomas was added to the cells and incubated for 2 h at room temperature. After four washing steps in NaCl/P_i-Tween, the cells were incubated simultaneously with anti- (mouse IgG) (1 : 2500) and anti-(mouse IgM) (1 : 2500) conjugated to horseradish peroxidase (HRP; Jackson ImmunoResearch Laboratories Inc., Baltimore Pike, PA, USA). After four additional washing steps, the bound monoclonal antibodies were detected by incubation with the HRP substrate tetramethylbenzidine and the reaction was stopped by the addition of an equal volume of 1 M H_2SO_4 and A_{450} was recorded.

Concentration and purification of monoclonal antibodies

For the initial experiments, hybridoma media was concentrated using Centriplus YM-50 (Millipore, Bedford, MA, USA). To avoid interference with nucleotidase assays, inorganic phosphate was removed by dialysis against modified Ringer buffer (120 mM NaCl, 5 mM KCl, 2.5 mM $CaCl_2$, 1.2 mM $MgSO_4$, 25 mM $NaHCO_3$, 10 mM dextrose, 80 mM Tris–HCl, pH 7.4) using dialysis tubing (BRL, Gaithersburg, MO, USA). For most experiments, monoclonal antibodies were purified using a Protein A Sepharose CL-4B column equilibrated with 50 mM Tris–HCl (pH 7.0). The hybridoma media was adjusted to 50 mM Tris–HCl (pH 7.0) and applied to the column. The column was then washed with 10 volumes of 50 mM Tris–HCl (pH 7.0) and IgG was eluted with 100 mM glycine (pH 3.0). The eluted fractions were immediately neutralized with 1 M Tris–HCl (pH 9.0). The protein concentration was determined by the Bradford technique [59].

Transient transfection and preparation of cell extracts

Both African green monkey kidney cells (COS-1 or COS-7) and HEK 293T cells were transfected with an expression vector (pcDNA3) containing the cDNA encoding individual NTPDases using lipofectamine (Invitrogen), as previously described [2]. Forty to seventy-two hours post-transfection, the cells were harvested, and cell extracts [22] or crude cell membranes [24] were obtained. Protein concentrations were estimated by the Bradford microplate assay using bovine serum albumin as the standard [59].

Immunoglobulin isotyping by dot blotting

Samples of 100 ng of goat IgG control (Cedarlane, Burlington, Canada), mouse IgG1, IgG2a and IgG2b (Sigma-Aldrich) and purified monoclonal antibodies (hN3-$B3_S$ and hN3-$H10_S$) diluted in 400 μL of NaCl/Tris were applied to a PVDF membrane (Millipore) using a dot blot apparatus. The membrane was then blocked for 1 h with 5% Blotto in NaCl/Tris containing 0.1% Tween 20. The membrane was subsequently probed with rat antibodies to mouse IgG1, 2a and 2b (a kind gift from M. P. Soares, BIDMC, HMS, Boston, MA, USA) at

1 : 200 dilution for 1 h, washed and incubated with ImmunoPure goat anti-(rat IgG) (H+L), peroxidase conjugated (Pierce Biotechnology, Rockford, IL, USA), at a concentration of 0.16 μg·mL^{-1} for 90 min followed by detection with the Chemiluminescent Reagent Plus kit (Perkin-Elmer Life Sciences, Boston, MA, USA).

Determination of antibody specificity

Western blotting—Protein samples were solubilized in NuPAGE lithium dodecyl sulfate sample buffer (Invitrogen), subjected to electrophoresis in NuPAGE 4–12% Bis-Tris gels under nonreducing conditions and electrotransferred to Immobilon-P membrane (Millipore). The membrane was blocked with 2.5% milk in NaCl/P_i-Tween overnight at 4 °C. It was subsequently incubated with hybridoma media diluted 1 : 10 in the above blocking buffer for 90 min, washed, and then incubated with HRP-conjugated goat anti-(mouse IgG) in 0.5% milk in NaCl/P_i-Tween (Jackson Immuno-Research Laboratories Inc.) for 60 min at dilution 1 : 10 000, followed by chemiluminescence detection as described above for dot blots.

Flow cytometry—HEK 293T cells transfected with human NTPDase3, as well as nontransfected cells used as controls, were detached from the plates with a citric saline solution (135 mM potassium chloride, 15 mM sodium citrate). Samples of 2×10^5 cells per tube were washed with an ice-cold PFA buffer (1% fetal bovine serum and 0.1% NaN_3 in NaCl/P_i) followed by incubation with or without the purified monoclonal antibody (hN3-$B3_S$ or hN3-$H10_S$) or control mouse IgG (I5381; Sigma-Aldrich) at a concentration of 1 μg·mL^{-1} in PFA for 30 min. After washes with PFA, the cells were incubated with Alexa FLUOR 633 F(ab′)$_2$ fragment of goat anti- (mouse IgG) (H+L) (Molecular Probes, Carlsbad, CA, USA) for 30 min on ice, washed with PFA, and analyzed by flow cytometry (EPICS XL; Beckman Coulter, Fullerton, CA, USA).

Immunocytochemistry, immunohistochemistry and enzyme histochemistry—COS-7 cells or sections (6 μm thick) of snap-frozen human pancreas (provided by B. Kunzlï, Department of General Surgery, University of Heidelberg, Heidelberg, Germany) were fixed in an ice-cold solution of 95% acetone and 5% of a 10% formalin solution (Fisher Scientific Co.) and blocked in a NaCl/P_i solution containing 7% normal goat serum for 30 min. For immunocytochemistry, COS-7 cells were incubated with the indicated hybridoma media overnight at 4 °C. For immunohistochemistry, pancreas tissue sections were incubated with mouse monoclonal anti-CD39 IgG1 (clone BU61; Ancell Corp., Bayport, MN, USA) or the mouse monoclonal anti-NTPDase3 IgG2b (hN3-$H10_S$) overnight at 4 °C. COS-7 cells or pancreas sections were then treated with 0.15% H_2O_2 in NaCl/P_i for 10 min to inactivate endogenous peroxidase, and with an avidin/biotin solution (Avidin/Biotin Blocking kit; Vector Laboratories, Burlington, Canada) to prevent nonspecific staining due to endogenous avidin/biotin. This step was followed by incubation with a secondary antibody from goat conjugated to biotin (Jackson ImmunoResearch Laboratories Inc.) at dilution 1 : 1000. The avidin-biotinylated HRP complex (VectaStain Elite ABC kit; Vector Laboratories) was added to optimize the reaction. Peroxidase activity was revealed using 3,3′-diaminobenzidine (Sigma-Aldrich) as substrate. Cells were counterstained with aqueous hematoxylin (Biomeda, Foster City, CA, USA) in accordance with the manufacturer's instructions.

Localization of ectonucleotidase activities was determined using the Wachstein/Meisel lead phosphate method [60]. In all assays, a 1 h incubation with 1 mM ATP as substrate was performed at 37 °C. To evaluate the inhibition efficiency of the monoclonal anti-NTPDase3 IgGs, fixed tissue sections were pre-incubated with hN3-H10$_S$ diluted in the appropriate buffer at the final concentration of 0.38 μg·mL^{-1} for 1 h at room temperature, prior to the addition of ATP and detection of nucleotidase activity.

Nucleotidase assays

Activity of cell lysates from NTPDase transfected COS-7 cells, depleted of nuclei by centrifugation, was determined as previously described [2,13]. Enzymatic reaction was performed at 37 °C in 0.2 mL of one of the three buffers, as indicated: modified Ringer buffer (120 mM NaCl, 5 mM KCl, 2.5 mM $CaCl_2$, 1.2 mM $MgSO_4$, 25mM $NaHCO_3$, 10 mM dextrose, 80 mM Tris–HCl, pH 7.4), Ca buffer (20 mM Mops, 5 mM $CaCl_2$, pH 7.4) or Mg buffer (20 mM Mops, 5 mM $MgCl_2$, pH 7.4). Cell extracts from human NTPDase1, 2, 3 or 8 transfected cells were added to the above incubation mixture and pre-incubated for 5 min at 37 °C. Where indicated, the purified monoclonal antibodies were pre-incubated for 20 min with the enzyme at a final concentration in the range 0.05–5000 ng·mL^{-1} IgG. Then, the reaction was initiated by the addition of 0.1 or 0.25 mM substrate (ATP or ADP), and terminated with 50 μL of the malachite green reagent after 10–15 min of hydrolysis. The inorganic phosphate released during the enzymatic reaction was measured as previously described with the malachite green assay [61]. The activity at the surface of intact cells was assayed in the modified Ringer buffer, as indicated above.

Epitope mapping and characteristics

SDS/PAGE and western blotting for epitope characterization—Pre-cast 15-well 4–15% gradient mini-gels (Bio-Rad, Foster City, CA, USA) were used for SDS/PAGE. Unless otherwise stated, the proteins were analyzed under nonreducing conditions to preserve the epitope recognized by monoclonal antibodies. To minimize the potential for disulfide exchange, 1 mM *N*-ethylmaleimide was included in the SDS sample loading buffer. In some experiments, proteins were run in the gels for approximately twice the time needed for the bromophenol blue dye to reach the bottom of the gels, allowing an improvement of the resolution in the molecular weight range of the NTPDase3 protein. After electrophoresis, the proteins were electrotransferred to Immun-Blot™PVDF membrane (Bio-Rad) and probed using a 1 : 5000 dilution of polyclonal rabbit antisera or a 1 : 5 dilution of hybridoma supernatant. After incubation overnight at 21 °C, the membrane was washed with buffer and a 1 : 2000 dilution of secondary IgGs conjugated to HRP [goat anti-(rabbit IgG) or goat anti-(mouse IgG) (10 μg·mL^{-1} stock concentration; Pierce Biotechnology)] was added, followed by incubation for 1–2 h at 21 °C. Immunoreactivity was detected by chemiluminescence using SuperSignal West Dura Extended Duration Substrate (Pierce Biotechnology), and was recorded using FluorChem IS-8800 system (Alpha Innotech, San Leandro, CA, USA) or Blue Autorad Film (BioExpress, Kaysville, UT, USA). Two rabbit polyclonal antibodies, KLH1 and KLH11, were generated against the C-terminal peptide (amino acid residues 515–529) and an internal peptide (amino acid residues 311–327) of human NTPDase3, respectively, as previously described [25,62]. KLH12 antibody was generated against another internal amino acid sequence of human NTPDase3

[(265)NEAEKKFLAMLLQNSPT(281)] and produced a weaker signal with NTPDase3 compared to KLH1 and KLH11 antibodies.

Site-directed mutagenesis of NTPDase3—Mutagenesis of the wild-type NTPDase3 in pcDNA3 vector was performed by using the QuikChange II site-directed mutagenesis kit (Stratagene, La Jolla, CA, USA). Mutations that disrupt each of five extracellular disulfide bonds have been made and described previously [25].

Site-directed cleavage of NTPDase3 with NTCB—To define the epitope location, we combined two techniques: (a) site-directed mutagenesis for introducing a cysteine residue into NTPDase3 at the desirable site of cleavage and (b) the subsequent chemical cleavage with NTCB at the introduced cysteine residue. The NTPDase3 fragments produced by site-directed cleavage were analyzed by western blotting for interaction with monoclonal antibodies. The reaction with NTCB was carried out in two steps, essentially as previously described [34]. In the first step, NTPDase3 in crude membrane preparations (60 μg of total membrane protein) was cyanylated with 0.5 mM NTCB in 0.1 M Tris–HCl (pH 8.0) for 30 min at 37 °C. In the second step, the pH of the samples was increased to 9.0 by adding 3 M Tris, and the cleavage was carried out by incubation for 20 h at 37 °C. The samples were either combined with nonreducing SDS sample loading buffer and analyzed by western blotting, or processed for the enrichment of NTPDase3 and its fragments by immobilized lectins. The latter procedure was needed due to the relatively low efficiency of cleavage, and the low affinity of the inhibitory monoclonal antibodies for NTPDase3 in western blotting, requiring increased amounts of NTPDase3 and its fragments to be used for the analyses. Due to glycosylation at multiple sites, both uncleaved NTPDase3 and its fragments were efficiently enriched using immobilized lectins. The remaining NTCB in samples was quenched by adding cysteine to a final concentration of 2 mM and incubating for 10 min at 21 °C. Samples were then combined with four volumes of 0.2% Triton X-100 in NaCl/Tris buffer (150 mM NaCl and 20 mM Tris–HCl, pH 7.5) and incubated for 15 min at 21 °C. The pH was adjusted to pH 7.5 by adding 1 M HCl, and the cell debris was removed by 5 min of centrifugation in a microcentrifuge. The supernatant of each sample (1.2 mL) was combined with 50 μL of a 50% bead slurry containing a 1 : 1 mixture of wheat germ lectin Sepharose 6MB (Pharmacia LKB Biotechnology AB, Uppsala, Sweden) and Con A Sepharose (Pharmacia LKB) beads. After 2 h of end-over-end rotation at 21 °C, the beads were pelleted by brief centrifugation and washed with 1 mL of 0.2% Triton X-100 in NaCl/Tris, followed by another wash with 1 mL of 50 mM Tris–HCl (pH 6.8). The proteins were extracted from beads by adding 25 μL of SDS sample loading buffer containing 1 mM NEM and boiling for 5 min. The samples were then analyzed by SDS/PAGE under nonreducing conditions.

Deglycosylation with endo-β-*N*-acetylglucosaminidase—Deglycosylation was performed using endo-β-*N*-acetylglucosaminidase (New England Biolabs, Beverly, MA, USA) according to the manufacturer's instructions. NTPDase3 in crude membrane preparations was combined with 10 × glycoprotein denaturing buffer (0.5% SDS, 1% β-mercaptoethanol final concentrations) and boiled for 10 min. The samples were then combined with the reaction buffer (New England Biolabs) and incubated with endo-β-*N*-acetylglucosaminidase at 37 °C for 3 h. The controls were incubated under the same

conditions, but without endo-β-*N*-acetylglucosaminidase. After incubation, the samples were combined with SDS loading buffer containing 200 mM dithiothreitol and analyzed by western blotting.

Slot blotting of COS cell membranes and an antibody binding assay—Binding of monoclonal antibodies to native NTPDase3 proteins was assayed using COS cell membranes immobilized on PVDF membrane by vacuum filtration. Aliquots of 200 μL of COS cell membranes diluted with NaCl/Tris were filtered in individual slots of a Bio-Rad Bio Dot SF slot blot apparatus. After washing the slots with NaCl/Tris buffer three times, the membranes were blocked with 5% milk in NaCl/Tris and processed as described above for western blots.

Statistical analysis

Statistical analysis was performed using EXCEL (Microsoft Corp., Redmond, WA, USA). Data are given as the mean ± SEM. A comparison between the experimental groups was made with Student's *t*-test. For all tests, $P < 0.05$ was considered statistically significant.

Acknowledgments

We thank Dr A. F. Knowles and Dr H. Zimmermann for providing the plasmids encoding for human NTPDase2 and rat NTPDase3, respectively. We also thank Dr S. Bourgoin for the kind gift of the monoclonal antibody against cytohesin (6D4-4) that was used as a negative control in some experiments. This work was supported by grants from the Canadian Institutes of Health Research (CIHR) to J. S., and from the National Institutes of Health (grants HL59915 and HL72882) to T. L. K. J. S. was also the recipient of a New Investigator award from the CIHR.

Abbreviations

ACR	apyrase conserved regions
HEK	human embryonic kidney
HRP	horseradish peroxidase
NTCB	2-nitro-5-thiocyanatobenzoic acid
NTPDase	NTP diphosphohydrolase
PVDF	poly(vinylidene difluoride)

References

1. Robson SC, Sévigny J, Zimmermann H. The E-NTPDase family of ectonucleotidases: structure, function, relationships and pathophysiological significance. Purinergic Signal. 2006; 2:409–430. [PubMed: 18404480]
2. Kukulski F, Lévesque SA, Lavoie EG, Lecka J, Bigonnesse F, Knowles AF, Robson SC, Kirley TL, Sévigny J. Comparative hydrolysis of P2 receptor agonists by NTPDases 1, 2, 3 and 8. Purinergic Signal. 2005; 1:193–204. [PubMed: 18404504]
3. Enjyoji K, Sévigny J, Lin Y, Frenette PS, Christie PD, Schulte Am Esch J II, Imai M, Edelberg JM, Rayburn H, Lech M, et al. Targeted disruption of CD39 /ATP diphosphohydrolase results in disordered hemostasis and thromboregulation. Nat Med. 1999; 5:1010–1017. [PubMed: 10470077]

4. Goepfert C, Sundberg C, Sévigny J, Enjyoji K, Hoshi T, Csizmadia E, Robson S. Disordered cellular migration and angiogenesis in cd39-null mice. Circulation. 2001; 104:3109–3115. [PubMed: 11748109]
5. Mizumoto N, Kumamoto T, Robson SC, Sévigny J, Matsue H, Enjyoji K, Takashima A. CD39 is the dominant Langerhans cell-associated ecto-NTPDase: modulatory roles in inflammation and immune responsiveness. Nat Med. 2002; 8:358–365. [PubMed: 11927941]
6. Sévigny J, Sundberg C, Braun N, Guckelberger O, Csizmadia E, Qawi I, Imai M, Zimmermann H, Robson SC. Differential catalytic properties and vascular topography of murine nucleoside triphosphate diphosphohydrolase 1 (NTPDase1) and NTPDase2 have implications for thromboregulation. Blood. 2002; 99:2801–2809. [PubMed: 11929769]
7. Jhandier MN, Kruglov EA, Lavoie EG, Sévigny J, Dranoff JA. Portal fibroblasts regulate the proliferation of bile duct epithelia via expression of NTPDase2. J Biol Chem. 2005; 280:22986–22992. [PubMed: 15799977]
8. Grenz A, Zhang H, Hermes M, Eckle T, Klingel K, Huang DY, Muller CE, Robson SC, Osswald H, Eltzschig HK. Contribution of E-NTPDase1 (CD39) to renal protection from ischemia-reperfusion injury. FASEB J. 2007; 21:2863–2873. [PubMed: 17442731]
9. Friedman DJ, Rennke HG, Csizmadia E, Enjyoji K, Robson SC. The vascular ectonucleotidase ENTPD1 is a novel renoprotective factor in diabetic nephropathy. Diabetes. 2007; 56:2371–2379. [PubMed: 17473221]
10. Deaglio S, Dwyer KM, Gao W, Friedman D, Usheva A, Erat A, Chen JF, Enjyoji K, Linden J, Oukka M, et al. Adenosine generation catalyzed by CD39 and CD73 expressed on regulatory T cells mediates immune suppression. J Exp Med. 2007; 204:1257–1265. [PubMed: 17502665]
11. Imai M, Kaczmarek E, Koziak K, Sévigny J, Goepfert C, Guckelberger O, Csizmadia E, Schulte Am Esch J II, Robson SC. Suppression of ATP diphosphohydrolase / CD39 in human vascular endothelial cells. Biochemistry. 1999; 38:13473–13479. [PubMed: 10521254]
12. Mishra SK, Braun N, Shukla V, Fullgrabe M, Schomerus C, Korf HW, Gachet C, Ikehara Y, Sévigny J, Robson SC, et al. Extracellular nucleotide signaling in adult neural stem cells: synergism with growth factor-mediated cellular proliferation. Development. 2006; 133:675–684. [PubMed: 16436623]
13. Lavoie ÉG, Kukulski F, Lévesque SA, Lecka J, Sévigny J. Cloning and characterization of mouse nucleoside triphosphate diphosphohydrolase-3. Biochem Pharmacol. 2004; 67:1917–1926. [PubMed: 15130768]
14. Kirley TL. NTPDase3. AfCS-Nature Molecule Pages. 2006; doi: 10.1038/mp.a003153.01
15. Belcher SM, Zsarnovszky A, Crawford AR, Hemani H, Spurling L, Kirley TL. Immunolocalization of ectonucleoside triphosphate diphosphohydrolase 3 in rat brain: implication for modulation of multiple homeostatic systems including feeding and sleep-wake behaviors. Neuroscience. 2005; 137:1331–1346. [PubMed: 16338080]
16. Appelbaum L, Skariah G, Mourrain P, Mignot E. Comparative expression of P2X receptors and ecto-nucleoside triphosphate diphosphohydrolase 3 in hypocretin and sensory neurons in zebrafish. Brain Res. 2007; 1174:66–75. [PubMed: 17868657]
17. Vlajkovic SM, Vinayagamoorthy A, Thorne PR, Robson SC, Wang CJ, Housley GD. Noise-induced up-regulation of NTPDase3 expression in the rat cochlea: Implications for auditory transmission and cochlear protection. Brain Res. 2006; 1104:55–63. [PubMed: 16815340]
18. Vekaria RM, Shirley DG, Sévigny J, Unwin RJ. Immunolocalization of ectonucleotidases along the rat nephron. Am J Physiol Renal Physiol. 2006; 290:F550–F560. [PubMed: 16189292]
19. Gendron FP, Halbfinger E, Fischer B, Duval M, D'Orleans-Juste P, Beaudoin AR. Novel inhibitors of nucleoside triphosphate diphosphohydrolases: chemical synthesis and biochemical and pharmacological characterizations. J Med Chem. 2000; 43:2239–2247. [PubMed: 10841802]
20. Gendron FP, Benrezzak O, Krugh BW, Kong Q, Weisman GA, Beaudoin AR. Purine signaling and potential new therapeutic approach: possible outcomes of NTPDase inhibition. Curr Drug Targets. 2002; 3:229–245. [PubMed: 12041737]
21. Muller CE, Iqbal J, Bagi Y, Zimmermann H, Rollich A, Stephan H. Polyoxometalates – a new class of potent ecto-nucleoside triphosphate diphosphohydrolase (NTPDase) inhibitors. Bioorg Med Chem Lett. 2006; 16:5943–5947. [PubMed: 16997558]

22. Munkonda MN, Kauffenstein G, Kukulski F, Lévesque SA, Legendre C, Pelletier J, Lavoie EG, Lecka J, Sévigny J. Inhibition of human and mouse plasma membrane bound NTPDases by P2 receptor antagonists. Biochem Pharmacol. 2007; 74:1524–1534. [PubMed: 17727821]
23. Lévesque SA, Lavoie EG, Lecka J, Bigonnesse F, Sévigny J. Specificity of the ecto-ATPase inhibitor ARL 67156 on human and mouse ectonucleotidases. Br J Pharmacol. 2007; 152:141–150. [PubMed: 17603550]
24. Smith TM, Kirley TL. Cloning, sequencing, and expression of a human brain ecto-apyrase related to both the ecto-ATPases and CD39 ecto-apyrases. Biochim Biophys Acta – Protein Struct Mol Enzymol. 1998; 1386:65–78.
25. Ivanenkov VV, Meller J, Kirley TL. Characterization of disulfide bonds in human nucleoside triphosphate diphosphohydrolase 3 (NTPDase3): implications for NTPDase structural modeling. Biochemistry. 2005; 44:8998–9012. [PubMed: 15966724]
26. Martín-Satué M, Lavoie EG, Pelletier J, Fausther M, Csizmadia E, Guckelberger O, Robson SC, Sévigny J. Localization of plasma membrane bound NTPDases in the murine reproductive tract. Histochem Cell Biol. 2009 in press.
27. Vorhoff T, Zimmermann H, Pelletier J, Sévigny J, Braun N. Cloning and characterization of the ecto-nucleotidase NTPDase3 from rat brain: predicted secondary structure and relation to other members of the E-NTPDase family and actin. Purinergic Signal. 2005; 1:259–270. [PubMed: 18404510]
28. Squires PE, James RF, London NJ, Dunne MJ. Characterization of purinergic receptor-evoked increases in intracellular Ca^{2+}transients in isolated human and rodent insulin-secreting cells. Purinergic receptor signalling and [Ca2+]i in human beta-cells. Adv Exp Med Biol. 1997; 426:173–179. [PubMed: 9544271]
29. Verspohl EJ, Johannwille B, Waheed A, Neye H. Effect of purinergic agonists and antagonists on insulin secretion from INS-1 cells (insulinoma cell line) and rat pancreatic islets. Can J Physiol Pharmacol. 2002; 80:562–568. [PubMed: 12117305]
30. Hellman B, Jansson L, Dansk H, Grapengiesser E. Effects of external ATP on Ca(2+) signalling in endothelial cells isolated from mouse islets. Endocrine. 2007; 32:33–40. [PubMed: 17992600]
31. Lavoie EG, Sévigny J. Localization of nucleoside triphosphate diphosphohydrolyse-3 in mouse digestive associated glands. Purinergic Signal. 2006; 2:245.
32. Chadwick BP, Frischauf AM. The CD39-like gene family – identification of three new human members (CD39L2, CD39L3, and CD39L4), their murine homologues, and a member of the gene family from *Drosophila melanogaster*. Genomics. 1998; 50:357–367. [PubMed: 9676430]
33. Kittel A, Pelletier J, Bigonnesse F, Guckelberger O, Kordas K, Braun N, Robson SC, Sévigny J. Localization of nucleoside triphosphate diphosphohydrolase-1 (NTPDase1) and NTPDase2 in pancreas and salivary gland. J Histochem Cytochem. 2004; 52:861–871. [PubMed: 15208353]
34. Degani Y, Patchornik A. Cyanylation of sulfhydryl groups by 2-nitro-5-thiocyanobenzoic acid. Highyield modification and cleavage of peptides at cysteine residues. Biochemistry. 1974; 13:1–11. [PubMed: 4808702]
35. Tang HY, Speicher DW. Identification of alternative products and optimization of 2-nitro-5-thiocyanatobenzoic acid cyanylation and cleavage at cysteine residues. Anal Biochem. 2004; 334:48–61. [PubMed: 15464952]
36. Murphy DM, Ivanenkov VV, Kirley TL. Identification of cysteine residues responsible for oxidative cross-linking and chemical inhibition of human nucleoside-triphosphate diphosphohydrolase 3. J Biol Chem. 2002; 277:6162–6169. [PubMed: 11748229]
37. Maley F, Trimble RB, Tarentino AL, Plummer TH Jr. Characterization of glycoproteins and their associated oligosaccharides through the use of endoglycosidases. Anal Biochem. 1989; 180:195–204. [PubMed: 2510544]
38. Helenius A, Aebi M. Intracellular functions of N-linked glycans. Science. 2001; 291:2364–2369. [PubMed: 11269317]
39. Smith TM, Kirley TL. Glycosylation is essential for functional expression of a human brain ecto-apyrase. Biochemistry. 1999; 38:1509–1516. [PubMed: 9931016]
40. Zimmermann H. Extracellular metabolism of ATP and other nucleotides. Naunyn Schmiedebergs Arch Pharmacol. 2000; 362:299–309. [PubMed: 11111825]

41. Gendron FP, Halbfinger E, Fischer B, Beaudoin AR. Inhibitors of NTPDase: key players in the metabolism of extracellular purines. Adv Exp Med Biol. 2000; 486:119–123. [PubMed: 11783467]
42. Iqbal J, Vollmayer P, Braun N, Zimmermann H, Muller CE. A capillary electrophoresis method for the characterization of ecto-nucleoside triphosphate diphosphohydrolases (NTPDases) and the analysis of inhibitors by in-capillary enzymatic microreaction. Purinergic Signal. 2005; 1:349–358. [PubMed: 18404519]
43. Knowles AF, Isler RE, Reece JF. The common occurrence of ATP diphosphohydrolase in mammalian plasma membranes. Biochim Biophys Acta. 1983; 731:88–96. [PubMed: 6303414]
44. Beaudoin, AR., Sévigny, J., Picher, M. ATP-diphosphohydrolases, apyrases, and nucleotide phosphohydrolases: biochemical properties and functions. In: Lee, AG., editor. ATPases. JAI Press Inc; Greenwich: 1996. p. 369-401.
45. Knowles AE, Nagy AK. Inhibition of an ecto-ATP-diphosphohydrolase by azide. Eur J Biochem. 1999; 262:349–357. [PubMed: 10336618]
46. Sévigny J, Picher M, Grondin G, Beaudoin AR. Purification and immunohistochemical localization of the ATP diphosphohydrolase in bovine lungs. Am J Physiol Lung Cell Mol Physiol. 1997; 272:L939–L950.
47. Sévigny J, Levesque FP, Grondin G, Beaudoin AR. Purification of the blood vessel ATP diphosphohydrolase, identification and localization by immunological techniques. Biochim Biophys Acta. 1997; 1334:73–88. [PubMed: 9042368]
48. Sévigny J, Robson SC, Waelkens E, Csizmadia E, Smith RN, Lemmens R. Identification and characterization of a novel hepatic canalicular ATP diphosphohydrolase. J Biol Chem. 2000; 275:5640–5647. [PubMed: 10681547]
49. Lemmens R, Vanduffel L, Kittel A, Beaudoin AR, Benrezzak O, Sévigny J. Distribution, cloning, and characterization of porcine nucleoside triphosphate diphosphohydrolase-1. Eur J Biochem. 2000; 267:4106–4114. [PubMed: 10866813]
50. Christoforidis S, Papamarcaki T, Galaris D, Kellner R, Tsolas O. Purification and properties of human placental ATP diphosphohydrolase. Eur J Biochem. 1995; 234:66–74. [PubMed: 8529670]
51. Fausther M, Lecka J, Kukulski F, Lévesque SA, Pelletier J, Zimmermann H, Dranoff JA, Sévigny J. Cloning, purification and identification of the liver canalicular ecto-ATPase as NTPDase8. Am J Physiol Gastrointest Liver Physiol. 2007; 292:G785–G795. [PubMed: 17095758]
52. Bigonnesse F, Lévesque SA, Kukulski F, Lecka J, Robson SC, Fernandes MJG, Sévigny J. Cloning and characterization of mouse nucleoside triphosphate diphosphohydrolase-8. Biochemistry. 2004; 43:5511–5519. [PubMed: 15122917]
53. Brunschweiger A, Iqbal J, Umbach F, Scheiff AB, Munkonda MN, Sevigny J, Knowles AF, Muller CE. Selective nucleoside triphosphate diphosphohydrolase-2 (NTPDase2) inhibitors: nucleotide mimetics derived from uridine-5′-carboxamide. J Med Chem. 2008; 51:4518–4528. [PubMed: 18630897]
54. Crawford AR, Gaddie KJ, Smith TM, Kirley TL. Characterization of an alternative splice variant of human nucleoside triphosphate diphosphohydrolase 3 (NTPDase3): a possible modulator of nucleotidase activity and purinergic signaling. Arch Biochem Biophys. 2007; 457:7–15. [PubMed: 17126282]
55. Zebisch M, Strater N. Structural insight into signal conversion and inactivation by NTPDase2 in purinergic signaling. Proc Natl Acad Sci USA. 2008; 105:6882–6887. [PubMed: 18458329]
56. Lavoie EG, Fausther M, Sévigny J. Regulation of insulin secretion by NTPDase3. Purinergic Signal. 2008; 4:S50.
57. Kaczmarek E, Koziak K, Sévigny J, Siegel JB, Anrather J, Beaudoin AR, Bach FH, Robson SC. Identification and characterization of CD39 vascular ATP diphosphohydrolase. J Biol Chem. 1996; 271:33116–33122. [PubMed: 8955160]
58. Knowles AF, Chiang WC. Enzymatic and transcriptional regulation of human ecto-ATPase / E-NTPDase 2. Arch Biochem Biophys. 2003; 418:217–227. [PubMed: 14522593]
59. Bradford MM. A rapid and sensitive method for quantification of microgram quantities of protein utilizing the principle of protein-dye binding. Anal Biochem. 1976; 72:248–254. [PubMed: 942051]

60. Braun N, Sévigny J, Mishra SK, Robson SC, Barth SW, Gerstberger R, Hammer K, Zimmermann H. Expression of the ecto-ATPase NTPDase2 in the germinal zones of the developing and adult rat brain. Eur J Neurosci. 2003; 17:1355–1364. [PubMed: 12713638]

61. Baykov AA, Evtushenko OA, Avaeva SM. A malachite green procedure for orthophosphate determination and its use in alkaline phosphatase-based enzyme immunoassay. Anal Biochem. 1988; 171:266–270. [PubMed: 3044186]

62. Smith TM, Kirley TL. Site-directed mutagenesis of a human brain ecto-apyrase: evidence that the E-type ATPases are related to the actin / heat shock 70 / sugar kinase superfamily. Biochemistry. 1999; 38:321–328. [PubMed: 9890913]

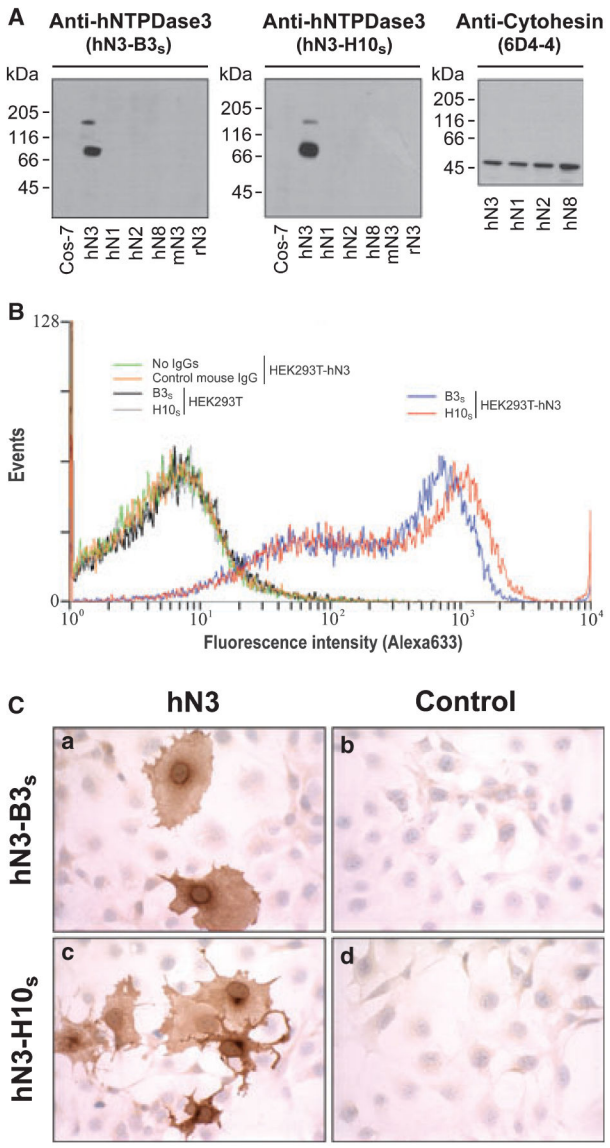

Fig. 1.

Specificity of the monoclonal antibodies hN3-B3$_S$ and hN3-H10$_S$ to human NTPDase3. (A) Western blotting: protein extracts from COS-7 cells transfected with human NTPDase3 (hN3), human NTPDase1 (hN1), human NTPDase2 (hN2), human NTPDase8 (hN8), mouse NTPDase3 (mN3) or rat NTPDase3 (rN3), as well as from membranes from nontransfected COS-7 cells, were subjected to electrophoresis in NuPAGE 4–12% Bis-Tris gels under nonreducing conditions and transferred to Immobilon-P membranes. The membranes were probed with monoclonal antibodies to human NTPDase3 (hN3-B3$_S$ or hN3-H10$_S$), or with a monoclonal antibody against cytohesin (6D4-4) as a loading control. Monoclonal antibodies against human NTPDase3 detected exclusively the expected monomeric (75 kDa) and dimeric (150 kDa) forms of human NTPDase3. (B) Flow cytometry analysis: the binding of the monoclonal antibodies to the native human NTPDase3 was evaluated with intact HEK 293T cells transfected with human NTPDase3 (HEK293T-hN3). In control experiments,

flow cytometry analysis was performed with nontransfected cells (HEK293T) with each monoclonal antibody, and also with HEK293T-hN3 cells using mouse IgGs. The detection was carried out using secondary antibodies conjugated to Alexa. Shifts in fluorescence intensity were observed exclusively with HEK293T-hN3 cells in the presence of either monoclonal hN3-$B3_S$ or hN3-$H10_S$ antibodies, demonstrating the specificity of the antibodies to human NTPDase3. (C) Immunocytochemistry: COS-7 cells transfected with a human NTPDase3 expression vector (hN3, left panels) and nontransfected COS-7 cells (control, right panels) were probed with the monoclonal antibodies, hN3-$B3_S$ (upper panels) or hN3-$H10_S$ (lower panels). Specific staining can be seen in human NTPDase3-transfected cells incubated with either monoclonal antibody (left panels) but not in nontransfected cells.

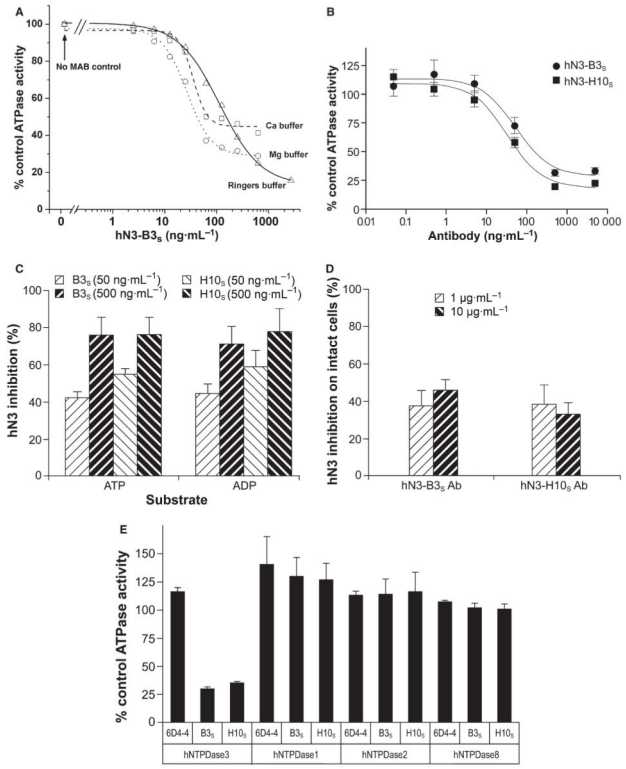

Fig. 2.

The mouse monoclonal antibodies hN3-B3$_S$ and hN3-H10$_S$ inhibit specifically and similarly the nucleotidase activity of human NTPDase3. Enzymatic activity assays were carried out with protein extracts from COS-7 cells transfected with human NTPDase3, or other NTPDases, as indicated. Unless indicated otherwise, the hydrolysis of 100 μ_M ATP or ADP in the presence of the indicated amount of purified monoclonal antibody was evaluated in Ringer buffer and the data presented are the mean ± SEM of at least six independent experiments, each carried out in triplicate. (A) Titration of the inhibition of ATPase activity by monoclonal hN3-B3$_S$ antibody in three buffers: Ca buffer, Mg buffer or Ringer buffer, as described in the Experimental procedures. In these assays, the substrate ATP was used at a final concentration of 0.25 mM. The results are expressed as percent of control activity in the absence of monoclonal antibody and are the average values from two sets of experiments. The fitted parameters derived from each set of averaged data are: Ca buffer, IC_{50} = 35 ± 4 ng·mL^{-1}, final % control activity = 45 ± 2%; Mg buffer, IC_{50} = 27 ± 3 ng·mL^{-1}, final % control activity = 29 ± 2%; Ringers buffer, IC_{50} = 113 ± 7 ng·mL^{-1}, final % control activity = 13 ± 2%. (B) Comparative dose–response inhibition curve of human NTPDase3 ATPase activity by hN3-B3$_S$ and hN3-H10$_S$ in Ringer buffer. A similar maximal inhibition is observed at 500 ng·mL^{-1} for either monoclonal antibody. (C) Comparative inhibition of human NTPDase3 activity by hN3-B3$_S$ and hN3-H10$_S$. The 100% activity of human NTPDase3 with ATP or ADP as substrate in Ringer was 271 ± 8 and 80 ± 5 nmol P_i·mg protein^{-1}·min^{-1}, respectively. (D) The monoclonal antibodies also inhibit the ATPase activity of NTPDase3 expressed at the surface of intact transfected cells. (E) Both monoclonal antibodies inhibit specifically human NTPDase3. At a concentration of 500

ng·mL^{-1}, neither hN3-B3$_S$ nor hN3-H10$_S$ inhibited human NTPDase1, 2 or 8. One hundred percent ATPase activity for NTPDase1, 2 and 8 corresponds to 93 ± 5, 198 ± 3 and 331 ± 98 nmol P_i·mg protein^{-1}·min^{-1}, respectively. Monoclonal antibody against cytohesin (6D4-4) served as a negative control.

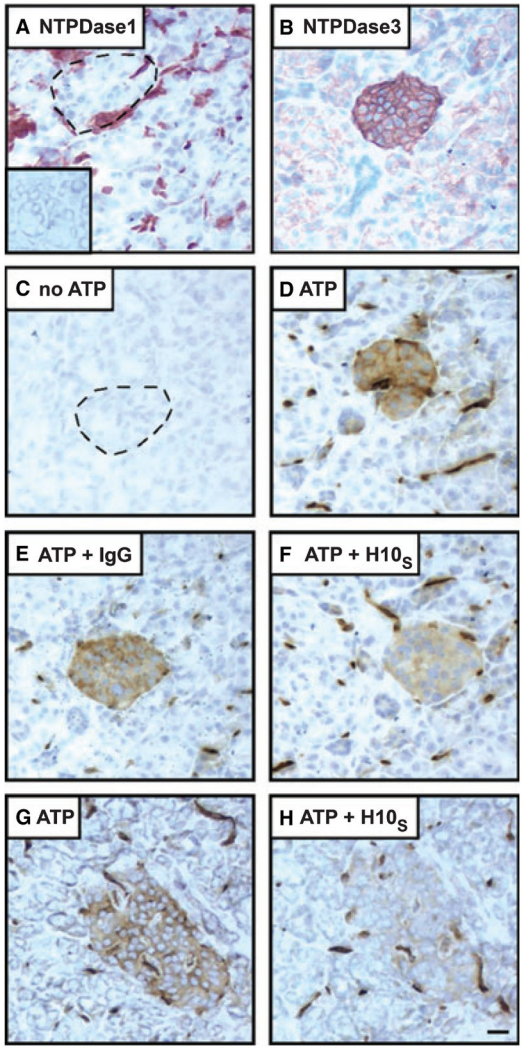

Fig. 3.

NTPDase3 is expressed in Langerhans islet cells of the human pancreas and is specifically inhibited *in situ* by hN3-H10$_S$. Two different groups of serial sections (A–F and G–H, respectively) were stained with the NTPDase1 monoclonal antibody BU61 (A) or with the NTPDase3 antibody hN3-H10$_S$ (B) or for ATPase activity in the presence (F, H) or absence (D, E, G) of hN3-H10$_S$. Counterstaining of nuclei (blue) was performed with aqueous hematoxylin. Where necessary for clarity of presentation, Langerhans islets are delimited by a dotted line (A, C). In all other panels, the islets can be easily distinguished. Note that there is a single islet on each of these panels. Although no staining can be seen in control sections incubated without primary antibody (A, inset), NTPDase1 expression is detected in blood vessels and capillaries, including those in Langerhans islets (A). By contrast, NTPDase3 immunostaining is detected in the pancreatic Langerhans islet cells (B). The presence of both of these enzymes together correlates with ATPase activity that can be seen in both of these structures (D, E, G). Control sections incubated without ATP displayed no staining (C). When the pancreas sections were pre-incubated with hN3-H10$_S$ antibody prior to the addition of the substrate ATP, its hydrolysis was significantly reduced in Langerhans islets

but not in blood vessels (F, H). Pre-incubation of pancreas sections with total mouse IgGs did not alter ATPase activity (E). Taken together, these results indicate that the monoclonal hN3-H10$_S$ antibody specifically inhibits *in situ* human NTPDase3 activity present in Langerhans islet cells. Scale bar = 20 μm.

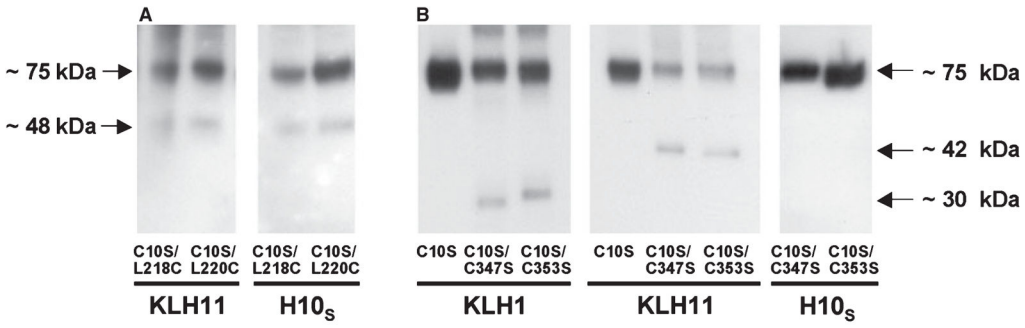

Fig. 4.

NTCB chemical cleavage at the introduced cysteine residues delineates the epitope location. To approximately localize the SDS-resistant epitope, we introduced cysteine residues into a C10S NTPDase3 background by mutagenesis, chemically cleaved the enzyme with NTCB at these cysteine residues, and analyzed the interaction of NTPDase3 fragments with monoclonal hN3-H10$_S$ antibody by western blotting under nonreducing conditions. (A) Cleavage with NTCB at Cys218 and Cys220 produced a fragment that contains the entire SDS-resistant epitope. Cysteine residues were introduced in the ACR4 by L218C and L220C mutagenesis. Cleavage with NTCB at these residues produces a fragment of approximately 48 kDa, which retains the full capability for binding monoclonal antibody on western blots. Thus, the monoclonal antibody epitope is located within the C-terminal fragment beginning at L220 in the sequence of NTPDase3. (B) Cleavage with NTCB at Cys347 and Cys353 destroys the monoclonal antibody epitope. The non-essential fourth disulfide bond was disrupted by either C347S or C353S mutation, thus producing an unpaired Cys353 or Cys347, respectively. Subsequent chemical cleavage produced two fragments of approximately 30 and 42 kDa, which are recognized by KLH1 and KLH11 antibodies, respectively. Note that neither cleavage fragment is recognized by the inhibitory monoclonal antibody, suggesting that the cleavage at either Cys347 or Cys353 splits two parts of the epitope, and that both of these parts are required for binding monoclonal antibody on western blots (the schematic representation of the locations of the polyclonal antibody binding sites and the cleavage sites are shown in Fig. 8A).

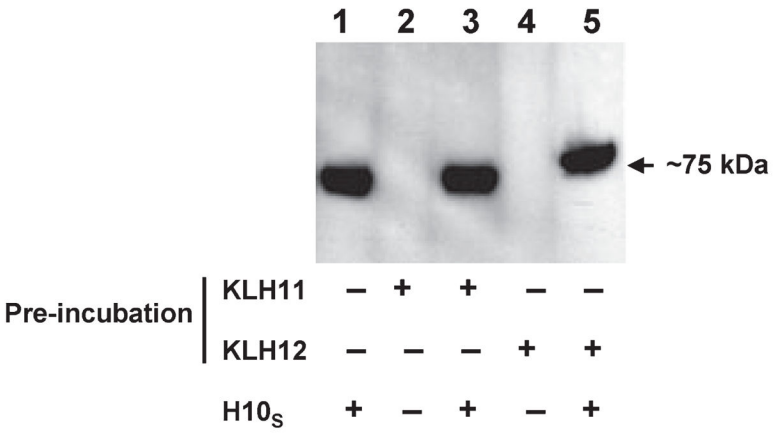

Fig. 5.

Lack of competition of the hN3-H10$_s$ monoclonal antibody with KLH11 and KLH12 affinity-purified polyclonal antibodies in western blots. Equal amounts of nonreduced C10S NTPDase3 were applied in each of five lanes. Membranes were pre-incubated with affinity-purified KLH11 (lanes 2 and 3) or KLH12 (lanes 4 and 5) antibodies (5 μg·mL^{-1} antibody in 5% nonfat milk in NaCl/Tris for 3 days at 4 °C). Lane 1 was pre-incubated in 5% nonfat milk in NaCl/Tris (no competing antibody). Then, a fresh aliquot of KLH11 or KLH12 antibody was added to raise the total concentration to 7 μg·mL^{-1} (to assure saturation with competing antibody), and affinity-purified monoclonal antibody hN3-H10$_s$ was added to a final concentration of 1 μg·mL^{-1} (lanes 1, 3 and 5). Following overnight incubation at 21 °C, all lanes were probed with secondary antibody [anti-(mouse IgG)], which recognizes hN3-H10$_s$, but not the polyclonal rabbit antibodies KLH11 and KLH12, as demonstrated by the lack of a signal in lanes 2 and 4. Monoclonal hN3-H10$_s$ antibody binding to NTPDase3 was not affected by pre-incubation with polyclonal KLH11 and KLH12 antibodies at high concentrations (compare lanes 1, 3 and 5), indicating that the monoclonal antibody epitope does not overlap with peptide sequences recognized by KLH11 and KLH12.

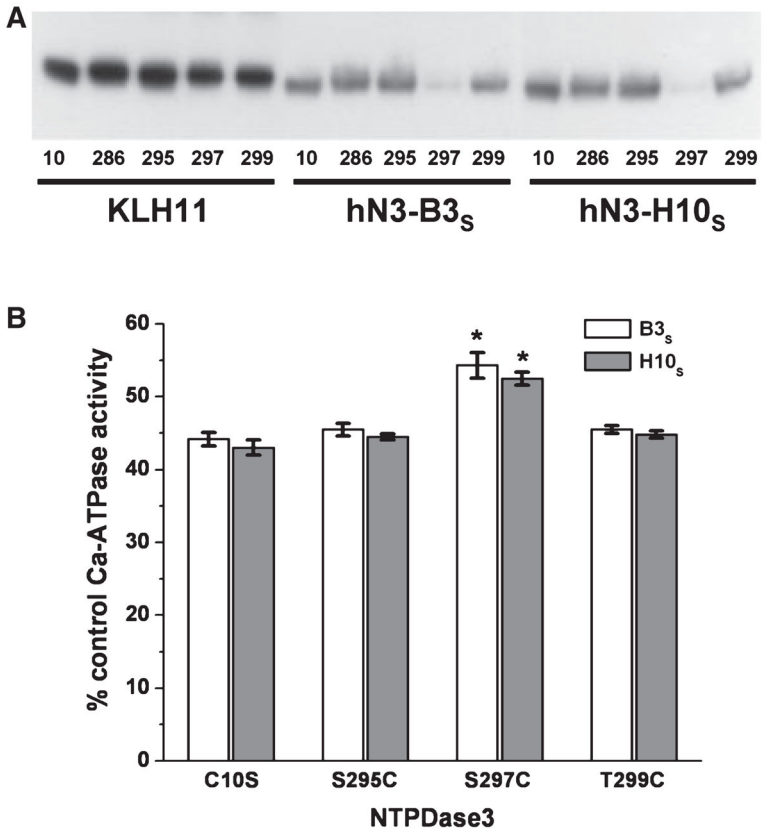

Fig. 6.

Effect of single amino acid substitutions on binding monoclonal antibody. All mutations were made in a C10S NTPDase3 background. (A) Effect of mutations on monoclonal antibody binding as analyzed by western blotting. The expression level of the S297C mutant is similar to that of other mutants in a C10S NTPDase3 background as estimated by probing western blots with the polyclonal KLH11 anti-peptide serum. However, this mutant shows a greatly reduced capability for binding by both monoclonal antibodies compared to other mutants. (B) Effects of three closely spaced, conservative, Ser or Thr to Cys mutations on the inhibition of human NTPDase3 Ca-ATPase activity by the monoclonal antibodies. Consistent with the reduced binding of the monoclonal antibodies to the S297C mutant shown in (A), the inhibition of this mutant by identical saturating amounts of monoclonal antibodies is also significantly reduced (results shown were obtained by assaying in Ca buffer). The fact that the effect of the S297C mutation on Ca-ATPase inhibition is less pronounced than the effect on western blot reactivity suggests that one or more additional epitope elements are involved in monoclonal antibody recognition of native NTPDase3, and that they are disrupted during treatment with SDS. The asterisks indicate significant differences ($P < 0.05$) versus the C10S NTPDase3 background measurements.

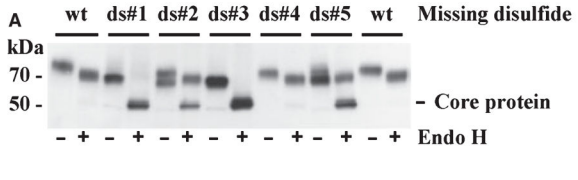

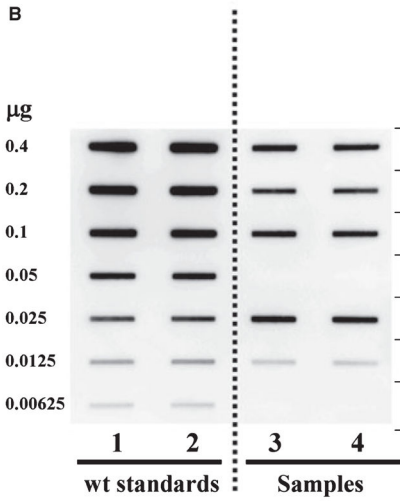

	Amount of loaded protein (µg)	Relative amount of properly folded protein	Density of signal with hN3-B3$_S$	Immuno-reactivity (density/properly folded protein)
wt	0.05	1	1	1
ds#1	0.2	~0.2	~0.6	~3
ds#2	0.2	1	0.9	0.9
ds#3	0.2	NA	NA	NA
ds#4	0.05	1	1	1
ds#5	0.2	1	0.13	0.13
pcDNA3 (blank)	0.2	NA	NA	NA

Fig. 7.

Significance of individual disulfide bonds for monoclonal antibody recognition of native human NTPDase3. (A) Estimation of the amount of properly folded and processed protein in the samples of wild-type (wt) and mutant NTPDase3 lacking one of each of the five disulfide bonds (ds#1, ds#2, ds#3, ds#4 and ds#5) by digestion with endo-β-*N*-acetylglucosaminidase followed by western blotting and detection with KLH11. We showed previously that the samples of mutant NTPDase3 contain variable amounts of misfolded and enzymatically inactive molecules, which possess immature glycans [25]. Treatment with endo-β-*N*-acetylglucosaminidase reduces the size of these misfolded molecules to that of the protein core of approximately 50 kDa. Thus, we estimated the amount of properly folded enzyme in each sample by quantitating the immunoreactive protein that remained in the 70 kDa band after treatement with endo-β-*N*-acetylglucosaminidase. Because of large variations in the relative amount of properly folded protein in the samples of mutated NTPDase3 compared to the wildtype, the protein amounts applied to the lanes were adjusted: 0.5 µg applied to the lanes corresponding to the wild-type and the mutant lacking the fourth disulfide bond (ds#4); 2 µg applied to all other lanes. This resulted in approximately equal amounts of properly folded protein of 70 kDa being resolved after treatment with endo-β-*N*-acetylglucosaminidase in the lanes corresponding to wt, ds#2, ds#4 and ds#5 samples. (B) The effect of disulfide bond disruption in NTPDase3 on hN3-B3s monoclonal antibody binding. Equivalent amounts of properly folded NTPDase3 proteins [immunoreactivity at 70 kDa after treatment with endo-β-*N*-acetylglucosaminidase, as shown in (A)] were subjected to slot blotting and probed with the monoclonal hN3-B3$_S$ antibody. A duplicate set of calibration standards loading the indicated amount of wild-type hNTPDase3 COS cell membranes are shown in lanes 1 and 2. Lanes 3 and 4 contain duplicate samples of wild-type hNTPDase3 and hNTPDase3 mutants lacking individual

disulfide bonds. Less properly folded NTPDase3 lacking ds#1 was loaded because loading an equivalent amount of mutant would exceed the total protein binding capacity of the slot blot PVDF membrane (results not shown). Also, an equivalent amount of properly folded protein for NTPDase3 lacking the ds#3 could not be loaded because there is no properly folded protein produced by expressing this mutation; see (A). The membrane preparation of COS cells transfected with the empty expression vector (pcDNA3) was analyzed as the blank control. The results indicate the importance of the fifth disulfide bond for monoclonal antibody recognition of native NTPDase3 on slot blot because the immunoreactivity relative to the amount of properly folded and processed protein is very low (0.13) for this mutant, in contrast to the other mutants lacking different individual disulfide bonds.

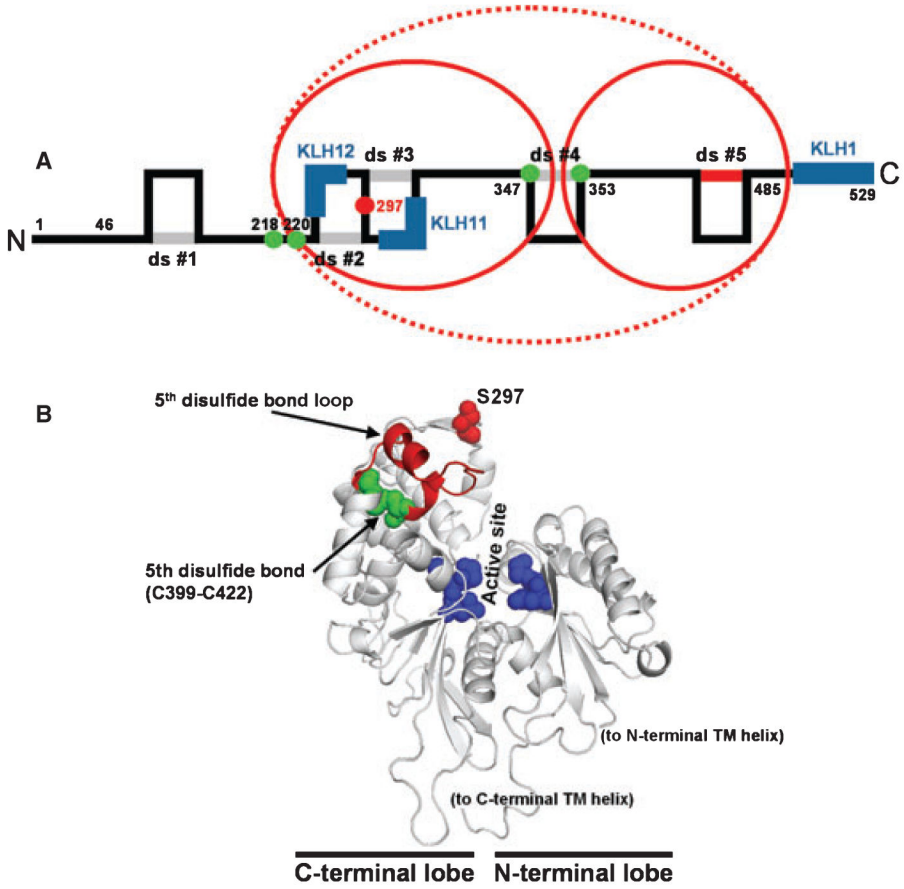

Fig. 8.

Linear and 3D model representations of inhibitory monoclonal antibody epitope mapping data. (A) Linear cartoon model of the human NTPDase3 sequence showing the location of the five disulfide bonds, important (numbered) amino acid residues, and binding and structural regions described in the present study. Human NTPDase3 consists of 529 amino acid residues. The extracellular portion of NTPDase3 (residues 46–485) contains five disulfide bonds (ds#1 to ds#5). KLH1, KLH11 and KLH12 are the binding sites for the polyclonal antibodies (shown in blue). Cleavage with NTCB at the introduced cysteine residues (Cys218 or Cys220) produced a C-terminal fragment capable of binding monoclonal antibodies. This locates the monoclonal antibody epitope within a fragment Leu220-Pro485 in the wild-type NTPDase3, as depicted by the dotted red oval. The non-essential fourth disulfide bond (ds#4) was disrupted by either C347S or C353S mutations, thus producing an unpaired Cys353 or Cys347 residue, respectively. The cleavage of these two mutants with NTCB produced two fragments, neither of which was recognized by monoclonal antibodies. This suggests that two parts of the epitope are located within two fragments, Leu220-Cys347 and Cys347-Pro485, as indicated by two solid red ovals. The lack of competition of monoclonal antibodies with polyclonal KLH11 and KLH12 antibodies excluded the KLH11 and KLH12 binding sites as the sites for monoclonal antibody binding. Site-directed mutagenesis identified Ser297 (shown in red) as a residue that likely interacts directly with the monoclonal antibodies. The disruption of the fifth

disulfide strongly diminished the interaction with both monoclonal antibodies, whereas the elimination of the first, second and fourth disulfides did not. This suggests that a principal part of the monoclonal antibody epitope is likely located near the fifth disulfide bond (shown in red). (B) A 3D model of the extracellular portion of human NTPDase3. The model was produced using the crystal structure of the extracellular portion of rat NTPDase2 [55] as the template for homology modeling, as described by Ivanenkov *et al.* [25]. The epitope localization data presented in this study are shown in this model along with the active site ACR1 and ACR4 'DXG' residues (depicted in blue space-filling mode). The location of the fifth disulfide bond is shown, with the two cysteines involved, C399 and C422, depicted in green space-filling mode in the C-terminal lobe of the model. The 22 amino acid loop bounded by the fifth disulfide bond is indicated in red. The data presented indicate that the monoclonal antibody epitope is located on the C-terminal lobe, contains S297 (shown in red space filling mode) and is dependent upon an intact fifth disulfide bond, perhaps due to proper positioning of amino acids in the fifth disulfide bond loop.